

Article

# On the Redox Activity of Urban Aerosol Particles: Implications for Size Distribution and Relationships with Organic Aerosol Components

Constantini Samara 

Environmental Pollution Control Laboratory, Department of Chemistry, Aristotle University of Thessaloniki, GR-54124 Thessaloniki, Greece; csamara@chem.auth.gr; Tel.: +30-2310-997805; Fax: +30-2310-997747

Received: 14 September 2017; Accepted: 18 October 2017; Published: 20 October 2017

**Abstract:** This article presents the distribution of the dithiothreitol-based (DTT) redox activity of water-soluble airborne particulate matter (PM) from two urban sites in the city of Thessaloniki, northern Greece in four size ranges (<0.49, 0.49–0.97, 0.97–3.0 and >3  $\mu\text{m}$ ). Seasonal and spatial variations are examined. The correlations of the mass-normalized DTT activity with the content of PM in water-soluble organic carbon (WSOC) and non-water-soluble carbonaceous species, such as organic and elemental carbon, as well as with solvent-extractable trace organic compounds (polycyclic aromatic hydrocarbons and nitro-derivatives, polychlorinated biphenyls, organochlorines, polybrominated biphenyl ethers) and polar organic markers (dicarboxylic acids and levoglucosan), are investigated. Our study provides new and additional insights into the ambient size distribution of the DTT activity of the water-soluble fraction of airborne PM at urban sites and its associations with organic PM components.

**Keywords:** DTT assay; solvent-extractable organic compounds; polar organic markers; size distribution; WSOC

## 1. Introduction

Exposure to particulate matter (PM) has been linked to adverse health effects such as respiratory and cardiovascular diseases and neurological disorders [1,2]. In most studies, effects were linked to  $\text{PM}_{10}$  or  $\text{PM}_{2.5}$  mass concentrations. However, smaller particles such as ultrafine particles (UFPs), i.e., particles with aerodynamic diameters <0.1  $\mu\text{m}$  and quasi-UFPs are of utmost significance from a public health viewpoint since they have higher pulmonary deposition efficiency and greater surface area, which increases their capacity to carry toxic chemicals [3,4].

Oxidative stress, resulting when the generation of reactive oxygen species (ROS), or free radicals, exceeds the available antioxidant defenses, has been suggested as an important underlying mechanism of action by which exposure to PM may lead to adverse health effects [5]. Oxidative potential of PM (i.e., the ability of particles to generate ROS), integrates various biologically relevant properties, including size, surface, and chemical composition; therefore, it may provide a more health-based exposure measure than PM mass alone and may be a better measure of the biologically effective dose that drives adverse health effects [6,7].

A number of different assays with different sensitivities to ROS generating compounds have been developed to quantify the oxidative potential of PM [7–11] with the dithiothreitol (DTT) assay being the most commonly used procedure [12]. DTT can be considered a chemical surrogate to cellular reductants, such as NADH or NADPH, which reduces  $\text{O}_2$  to superoxide anion ( $\text{O}_2^-$ ) and induces oxidative stress [13]. The electron transfer from DTT to oxygen is monitored by the rate at which DTT is consumed under a standardized set of conditions, and the rate is proportional to the concentration of the redox-active species in the PM sample [14,15].

Several *in vitro* studies have shown that the chemical oxidative potential of PM identified by the DTT consumption is directly related to its ability to induce cellular oxidative stress responses [16]. Significant correlation between DTT activity and *in vitro* MTT (3-(4,5-dimethylthiazol-2-yl)-2,5-diphenyltetrazolium bromide, an indicator of cellular metabolic activity) cytotoxicity was found in murine macrophages (RAW 264.7 cells) [17] and in human lung cells MRC-5 [18].

It is not clear so far which fraction (water-soluble or water-insoluble) contributes most to the oxidative potential of ambient or source PM. According to Verma et al. (2012) [19], most of the DTT activity of diesel particles occurs in their water-insoluble fraction. Furthermore, as revealed by Verma et al. (2015) [20], the DTT activity of the hydrophobic fraction of water-soluble PM<sub>2.5</sub> extracts was generally higher than those of the hydrophilic fraction accounting for 45–85% of total water-soluble DTT activity. Studies also indicated that, for ambient PM samples, methanol extracts produce significantly higher DTT reactivity in comparison to water extracts, due to the higher efficiency of methanol for both hydrophilic species and hydrophobic organic compounds [19,21,22]. The DTT activity of solvent-extractable PM measured after extraction with CH<sub>2</sub>Cl<sub>2</sub>/n-C<sub>6</sub>H<sub>14</sub>, fractionation and final solvent change to DMSO, followed the order: medium-polar organic fraction containing PAHs > non-polar organic fraction containing n-alkanes, PCBs, and OCPs > polar organic fraction containing NPAHs [23,24]. Nevertheless, in the majority of studies, the DTT activity of ambient PM has been measured in aqueous suspensions [12,17,25–27], and most frequently in aqueous extracts of PM filters [18,19,28–30].

Though the DTT assay is widely used, it is largely unknown which PM components are active in the DTT assay. PM components identified as DTT-active are quinones [13,31,32], humic-like substances (HULIS) [19,33], and dissolved transition metals [31]. The contributions to the resulting DTT response depend on the relative amounts of redox-active species. Verma et al. (2015) [20], estimated that organic compounds (mainly HULIS, which include highly oxidized organic compounds) contributed approximately 60% to the DTT activity of water-soluble PM<sub>2.5</sub> extracts, with the remaining probably due to water-soluble metals, which were mostly associated with the hydrophilic DTT fraction. Other studies, however, have emphasized the role of transition metals estimating that, for typical PM<sub>2.5</sub> samples, approximately 80% of DTT loss is from transition metals (especially Cu and Mn), while quinones accounted for approximately 20% [31]. Recently, it was demonstrated that sulfate plays a key role in producing highly acidic fine aerosols capable of dissolving primary transition metals that contribute to aerosol oxidative activity [34].

Source apportionment studies have been carried out to identify the sources of the DTT activity in ambient PM. Secondary organic carbon (SOC), primary biogenic emissions, and vehicular abrasion were the major sources driving the DTT activity of PM<sub>2.5</sub> in central Los Angeles, while the DTT activity of PM<sub>0.18</sub> was driven mainly by vehicle tailpipe emissions and vehicular abrasion [27]. Light-duty gasoline vehicles (LDGV) followed by biomass burning and heavy-duty diesel vehicles (HDDV) were found to be the major contributor to the DTT activity of PM<sub>2.5</sub> in Atlanta, GA [35]. Vehicular emissions (LDGV and HDDV), biomass burning, and secondary processes dominated the DTT activity of PM<sub>2.5</sub> in the southeastern United States [36]. Correspondingly, the major sources of DTT activity of PM<sub>0.49</sub> in Thessaloniki, Greece were vehicle exhaust at the urban traffic site and wood burning at the urban background site, with the contribution of the latter exceeding 80% during winter [28].

The present study is an extension of our previous efforts to link the redox activity of ambient PM to its characteristics such as size, location, and chemical composition. The water-soluble DTT activity of size-segregated PM (<0.49, 0.49–0.97, 0.97–3, and >3 μm) from two urban sites (urban traffic, UT and urban background, UB) in Thessaloniki, Greece, has been recently reported [18]. The aim of the present study was to assess the association of the DTT activity with solvent-extractable organic components including trace organic compounds, such as polycyclic aromatic hydrocarbons (PAHs) and PAH nitro-derivatives (NPAHs), polychlorinated biphenyls (PCBs), organochlorine pesticides (OCPs),

and polybrominated diphenyl ethers (PBDEs), as well as polar organic markers such as dicarboxylic acids (DCAs) and levoglucosan.

## 2. Experiments

### 2.1. Size-Segregated PM Samples

Size-resolved PM samples were collected from two urban sites (urban-traffic, UT and urban-background, UT), in the city of Thessaloniki, northern Greece (40°62' N, 22°95' E) during the cold (January–March 2013) and the warm (May–July 2013) period of the year. Sampling method has been described in detail elsewhere [18,37]. Briefly, 48-h size-segregated PM samples were collected using a five-stage high-volume cascade impactor (effective cut-off diameters at 7.2, 3.0, 1.5, 0.97, and 0.49  $\mu\text{m}$ ) and prebaked quartz filters. After all, some of the particle fractions obtained during each sampling event were merged so as to have four particle fractions (<0.49, 0.49–0.97, 0.97–3, and >3.0  $\mu\text{m}$ ) for further chemical analysis and redox activity measurements.

### 2.2. DTT Assay

The DTT analysis explicitly followed the method described by Cho et al. [12]. The DTT assay was conducted manually according to the procedure described elsewhere [18]. Briefly, PM filter samples were extracted in an ultrasonic bath using ultra-pure MilliQ water and the extracts were then filtered (0.45  $\mu\text{m}$  PTFE filters, Alltech, Nicholasville, KY, USA) to remove insoluble materials. The water extracts were incubated in duplicate at 37 °C for fixed time intervals (0, 20 and 40 min) to allow DTT consumption. The remaining DTT was allowed to react with 5,5'-dithiobis-2-nitrobenzoic acid (DTNB) to form 5-mercapto-2-benzoic acid which was monitored spectrophotometrically at 412 nm. The data collected at the multiple time points were used to determine the rate of DTT consumption which was normalized to the quantity of PM used in the incubation mixture. As regards quality control samples, both method blanks and positive control (9,10-phenanthrenequinone, PQN) were prepared and analyzed at the same time as the unknown samples. The mass-normalized DTT activity was expressed as  $\text{nmol min}^{-1} \mu\text{g}^{-1}$ .

### 2.3. Determination of WSOC and Particulate Carbonaceous Species

WSOC was extracted in an ultrasonic bath using ultra pure MilliQ water. The extracts were then filtered (0.45  $\mu\text{m}$  PTFE filters, Alltech) to remove insoluble materials, and WSOC was determined in a Shimadzu TOC-VCSH Analyzer using the Non Purgeable Organic Carbon (NPOC) method [38].

Particulate carbonaceous species (OC, EC) were measured using the thermal optical transmission (TOT) method following the NIOSH (National Institute for Occupational Safety and Health) 870 protocol, as described in [39]. Due to the lack of adequate amount of PM sample from slotted filters, OC and EC were measured only in the <0.49  $\mu\text{m}$  particle mode.

### 2.4. Extraction and Analysis of Trace Organic Compounds and Polar Organic Markers

The extraction and analysis of trace organic compounds and polar organic markers is previously described [37,40]. Briefly, filter segments were extracted with DCM/n-hexane (3:2 *v/v*) in a microwave-assisted extraction unit and PCBs/OCPs, PAHs and NPAHs were fractionated on a glass open chromatography column using sequentially n-hexane (non-polar organic fraction), DCM/n-hexane 3:2 *v/v* (moderately polar organic fraction), and acetone/n-hexane (3:7 *v/v*) (polar organic fraction), respectively. PBDEs were extracted from separate filter segments according to a more intensive procedure [37] including microwave assisted extraction with DCM/n-hexane (1:1 *v/v*), treatment with concentrated  $\text{H}_2\text{SO}_4$ , clean up through a glass column packed with acidic and neutral silica gel, and fractionation through an activated silica column. All trace organic compounds were analyzed by GC-MS operating in electron impact ionization (70 eV) and selected monitoring (SIM) mode [37,40]. Fifteen PCBs (-28, -31, -52, -101, -77, -105, -118, -126, -128, -156, -138, -153, -169, -170 and

-180), 18 OCPs ( $\alpha$ -HCH, HCB,  $\gamma$ -HCH,  $\beta$ -HCH, heptachlor, aldrin, isobenzan, isodrin, cis-heptachlor, o,p' DDE, endrin, p,p' DDE, o,p' DDD, dieldrin,  $\beta$ -endosulfan, p,p' DDD, o,p' DDT and p,p' DDT), 12 PAHs (Ph, An, Fl, Py, B[a]An, Chry, B[b]Fl, B[k]Fl, B[a]P, dB[a,h]An, B[ghi]Pe, I[1,2,3-cd]Py), 7 NPAHs (1-NNp, 2-NNp, 5-NAce, 3-NBPHE, 4-NBPHE, 3-NFl and 1-NPy), and 12 PBDEs (-15, -17, -28, -49, -71, -47, -66, -100, -99, -154, -153 and -183) were quantified in the extracts of the size segregated samples with variable frequencies (5–100%).

Due to the lack of adequate amount of PM sample from slotted filters, polar organic marker compounds such as low molecular weight dicarboxylic acids (DCAs) and anhydrosaccharides were measured only in the  $<0.49 \mu\text{m}$  particle fraction. DCAs (glycolic, malonic, maleic, succinic, glutaric, malic, salicylic, benzoic,  $\alpha$ -ketoglutaric, and phthalic) and the anhydrosugar levoglucosan, were analyzed by GC-MS after derivatization with BSTFA/TMCS after ultrasonic extraction of 1/4 of backup filters in DCM/methanol (2:1 *v/v*) [41].

### 2.5. Statistical Analysis

All descriptive statistics were computed using SPSS, version 24 (IBM company, Chicago, IL, USA). As both DTT activity and most organic PM components exhibited non-normal distributions in the Kolmogorov–Smirnov test, Spearman's rank correlation coefficients were mainly calculated to explore the association of individual chemical species with the DTT redox activity measured at the two sampling sites. Pearson correlation coefficients were also calculated for those chemical species following normal distribution. A *p* value  $< 0.05$  was considered significant.

## 3. Results and Discussion

### 3.1. Oxidative Potential of PM

#### 3.1.1. DTT Activity Levels

The time series of the mass-normalized DTT activity measured during the cold and the warm period in the different particle size fractions from the two urban sites is shown in Figure 1.

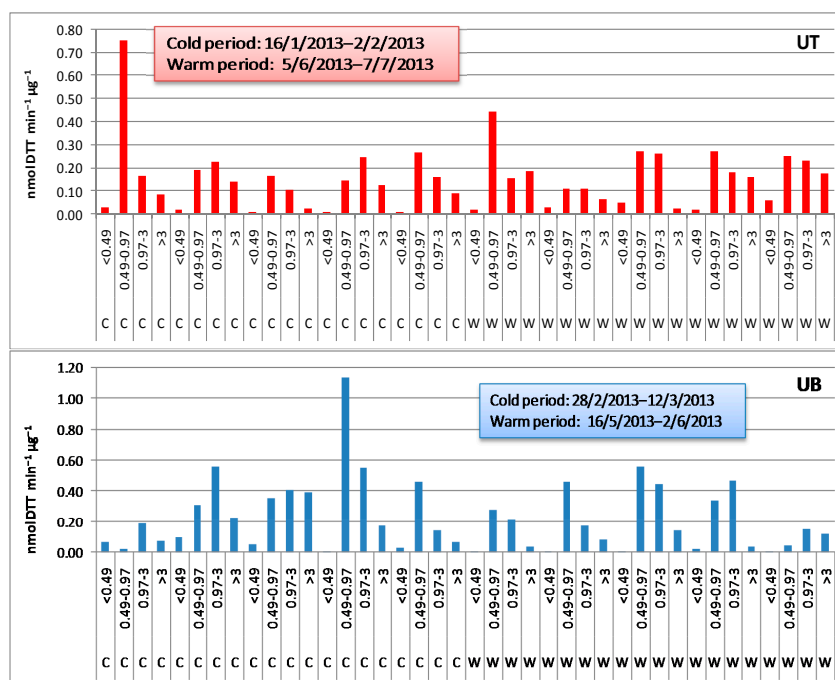


**Figure 1.** Mass-normalized DTT activity of the various particle size fractions (UT: urban traffic site; UB: urban background site; C: cold period; W: warm period).

The average ( $n = 5$ ) DTT activity of the different particle fractions ranged within 0.016–0.306 and 0.036–0.271  $\text{nmol min}^{-1} \mu\text{g}^{-1}$  at the UT site vs. 0.052–0.459 and 0.012–0.340  $\text{nmol min}^{-1} \mu\text{g}^{-1}$  at the UB site in the cold and the warm period, respectively. These activities are towards the highest end of the range of values reported in literature, which, however, are referred mostly to ordinary particle size fractions such as  $\text{PM}_{2.5}$ ,  $\text{PM}_{10}$ , or  $\text{PM}_{2.5-10}$  (Table 1).

**Table 1.** Mass-normalized DTT activity of ordinary PM fractions.

| DTT Activity ( $\text{nmol min}^{-1} \mu\text{g}^{-1}$ ) | Particle Size Fraction | Reference |
|--|------------------------|-----------|
| 0.015 ± 0.008  | $\text{PM}_{2.5}$      | [29]      |
| 0.011 ± 0.007  | $\text{PM}_{10}$       | [29]      |
| 0.015–0.070  | $\text{PM}_{2.5}$      | [31]      |
| 0.02–0.06  | $\text{PM}_{10}$       | [42]      |
| 0.005–0.1  | $\text{PM}_{2.5}$      | [36]      |
| 0.03–0.18  | $\text{PM}_{2.5}$      | [43]      |
| 0.33–3.43  | TSP                    | [44]      |
| 0.020–0.045  | $\text{PM}_{2.5}$      | [27]      |
| 0.020–0.06   | $\text{PM}_{0.18}$     | [27]      |
| 0.010–0.038  | $\text{PM}_{2.5}$      | [45]      |
| 0.007–0.028  | $\text{PM}_{2.5-10}$   | [45]      |
| 0.03–0.11  | $\text{PM}_{0.25}$     | [26]      |
| 0.010–0.666  | $\text{PM}_{0.18}$     | [17]      |
| 0.030–0.617  | $\text{PM}_{2.5}$      | [17]      |
| 0.022–0.484  | $\text{PM}_{2.5-10}$   | [17]      |

The DTT activity of PM emitted from diesel and gasoline vehicles has been measured under various driving cycles and fuels. Geller et al. (2006) [46], found relatively higher DTT activity for diesel than gasoline transient driving ( $0.039 \pm 0.05$  vs.  $0.025 \pm 0.03$   $\text{nmol min}^{-1} \mu\text{g}^{-1}$  of PM mass emitted) with the highest values been found in the DPF-equipped diesel vehicle ( $0.110 \pm 0.02$   $\text{nmol min}^{-1} \mu\text{g}^{-1}$  of PM mass emitted).

### 3.1.2. Size Distribution of DTT Activity

A summary of the spatial and seasonal trends in the mean DTT activity of each particle size fraction has been shown in a previous publication [18]. These data are reproduced in Figure 2 along with the PM mass concentration in each size range.

Apparently, regardless of site and season, the mean DTT activity maximized in the 0.49–0.97  $\mu\text{m}$  particle fraction decreasing onwards almost linearly with increasing particle size. A similar decreasing trend with particle size was previously found for the solvent-extractable DTT activity of size segregated PM in Thessaloniki, with highest values in the submicron mode  $<0.95 \mu\text{m}$  [23,24].

Apparently, the lowest DTT activity occurred in fraction  $<0.49 \mu\text{m}$  implying that the quasi-UFP mode, that accounted for 57% and 53% of the bulk PM mass at the UT and the UB site, respectively (Figure 2b) are less enriched with water-soluble DTT-active substances than larger particles. The higher DTT activity of the upper submicron mode compared to the  $<0.49 \mu\text{m}$  mode is in agreement to Charrier et al. (2015) [47], who found that submicron fine PM ( $0.17 \mu\text{m} \leq D_p \leq 1.0 \mu\text{m}$ ) typically has a larger mass-normalized oxidative potential than UFPs ( $\text{PM}_{0.17}$ ).

It is generally found that  $\text{PM}_{2.5}$  has higher intrinsic DTT activity than  $\text{PM}_{10}$  [25,29,43,45,48]. However, while some studies found higher intrinsic DTT activity in quasi-UFP particles than in  $\text{PM}_{2.5}$  [14,27,49], the opposite was reported by Steenhof et al. [17] for several sites. Similarly, while some studies found higher DTT activity in quasi-UFP mode particles ( $<0.18 \mu\text{m}$ ) than in accumulation ( $0.18$ – $2.5 \mu\text{m}$ ) and coarse fractions ( $>2.5 \mu\text{m}$ ) [12,25], Hu et al. [50] found rather low variability among the three size ranges studied ( $<0.25$ ,  $0.25$ – $2.5$  and  $2.5$ – $10 \mu\text{m}$ ). Information concerning the ambient size distribution of DTT activity is limited. Recently, Fang et al. (2017) [51] studying the distribution of water-soluble DTT activity in ten size fractions within the range  $0.056$ – $18 \mu\text{m}$ , found that, at the roadside

site, the highest values were in the 0.1–0.18  $\mu\text{m}$  fraction followed by the 10–18  $\mu\text{m}$  fraction, while the urban background exhibited highest values in the 0.1–0.18, 0.056–0.1 and 10–18  $\mu\text{m}$  size ranges.

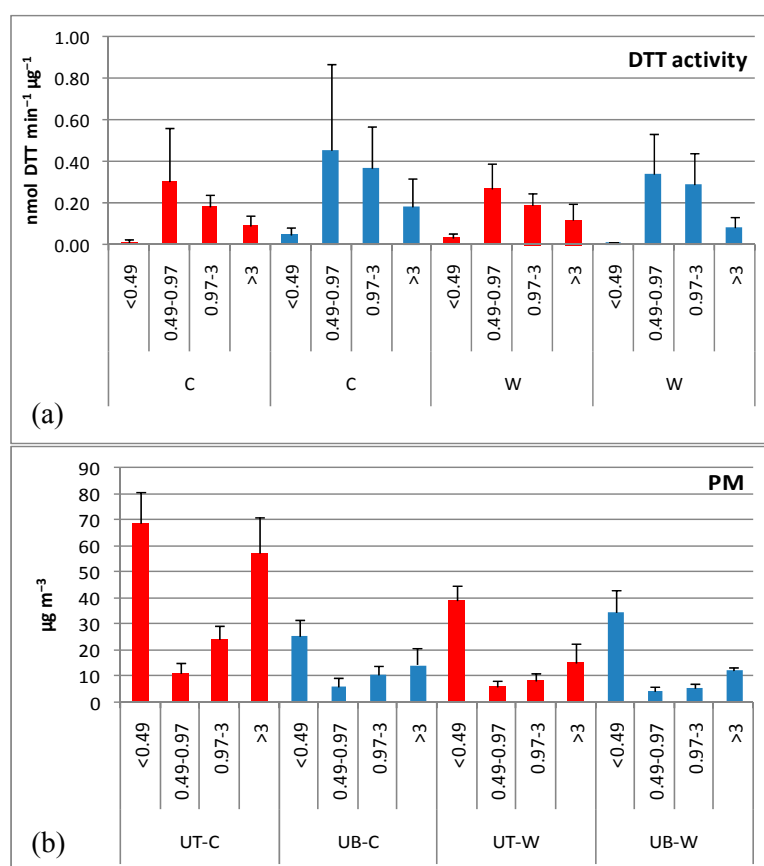


**Figure 2.** Mean  $\pm$  SD of (a) the DTT activity of size-segregated PM, (b) the concentrations of size-segregated PM (UT: urban traffic site; UB: urban background site; C: cold period; W: warm period).

### 3.1.3. Seasonal and Spatial Variations

The spatiotemporal variability of DTT may provide information on the variation of DTT-active chemical components [52].

In most particle size fractions, DTT activity showed more pronounced seasonal variability at the UB site (Figure 2) with cold/warm ratios noticeably higher compared to the UT site (4.3, 1.3, 1.3, 2.2 vs. 0.4, 1.1, 1.0, 0.8 in size fractions <0.49, 0.49–0.97, 0.97–3 and >3  $\mu\text{m}$ , respectively). Higher wintertime DTT activity has been frequently reported [9,24,26,27,36,53], on the contrary, other studies found higher activity in summer as compared to winter [31,44,47].

Elevated DTT levels in winter are mainly attributed to the increased particle-phase partitioning of semi-volatile organic compounds, which have been shown to be DTT-active [25,30], as well as their higher concentration due to the lower mixing height of the atmosphere during the cold periods. Studies have reported a decreased PM-induced DTT activity at high temperatures due to significant evaporative losses of volatile and semivolatile organic compounds (most notably PAHs) [30,52]. The higher redox potential found in all particle fractions from UB in winter could therefore be attributed to the increased biomass burning emissions at this site that are associated with high PAHs levels [54]. Conversely, the higher summertime redox potential of particles <0.49 and >3  $\mu\text{m}$  at UT could be related to fresh traffic emissions and traffic-induced resuspension of road dust, respectively.

In our study, it appears that the seasonal contrast varies in the different particle modes being larger in the <0.49  $\mu\text{m}$  mode. Charrier et al. (2015) [47] also found that the DTT activity of submicron

fine PM ( $0.17 \mu\text{m} \leq D_p \leq 1.0 \mu\text{m}$ ) was 61% higher in summer compared to winter, while UFPs ( $\text{PM}_{0.17}$ ) exhibited similar oxidative potential between seasons.

DTT activity is impacted by both local emissions associated by individual site characteristics and regional sources [36]. Some field studies carried out at different locations, with different contributing sources, found higher DTT activity at continuous traffic and underground sites [43], and/or near freeways [24]. Conversely, other studies found spatially uniform DTT activity [36,44,49]. In our study—excepting summertime particle fractions  $<0.49$  and  $>3 \mu\text{m}$ , which exhibited higher DTT activity at the UT site, thus suggesting the dominant contribution of traffic emissions—DTT activity was higher at the UB site. This could be attributed to the increased biomass burning at the UB site [54].

### 3.2. Carbonaceous Content of PM

The WSOC content of the size segregated PM exhibited different size distribution pattern at the two sites (Figure 3a). At UT, it was monomodal in both seasons peaking in  $0.49\text{--}0.97 \mu\text{m}$ . In contrast, at UB, a bimodal distribution was found with a first peak in  $<0.49 \mu\text{m}$  in both seasons, and an additional peak in  $0.97\text{--}3 \mu\text{m}$  in winter. Association of WSOC with the quasi-ultrafine particles suggests that gas-to-particle conversion of anthropogenic VOCs may be an important secondary formation pathway. Correspondingly, the high WSOC content of wintertime supermicronic particles from UB could be attributed to biomass burning emissions that are characterized by larger and highly water-soluble particles compared with those emitted from fossil fuel combustion [54]. The intra-site differences were larger in summer with all particle size fractions exhibiting higher WSOC content at UT compared with UB; in contrast, in winter, differences were smaller with UB exceeding UT in  $<0.49$  and  $0.97\text{--}3 \mu\text{m}$  size fractions.

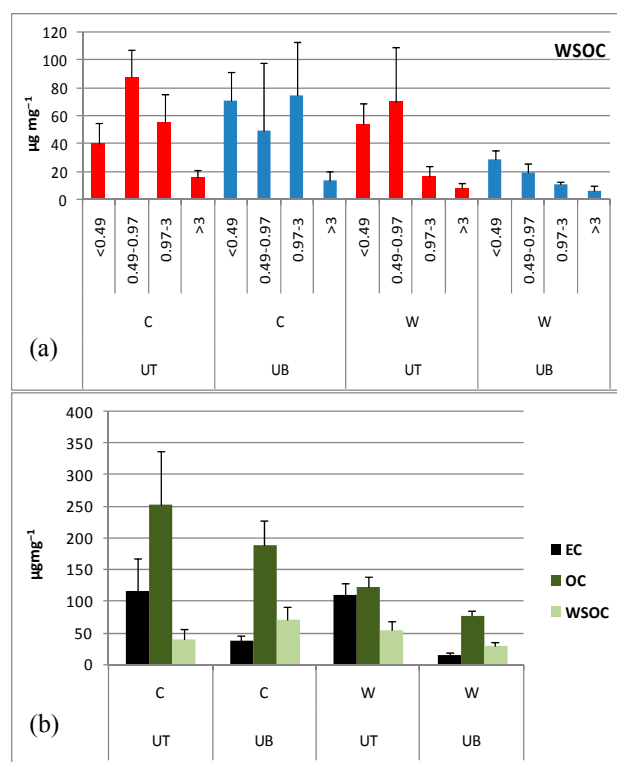


**Figure 3.** Mean  $\pm$  SD of (a) the WSOC content in size-segregated PM, (b) the content of carbonaceous species in the  $<0.49 \mu\text{m}$  particle fraction (UT: urban traffic site; UB: urban background site; C: cold period; W: warm period).

Although WSOC may decrease in winter due to enhanced wet depositional losses [49], the WSOC content of all PM size fractions was higher in winter with cold/warm ratios 2.4, 2.5, 6.2 and 2.2,

respectively at UB vs. 0.7, 1.3, 3.3 and 1.9 at UT. The larger summertime WSOC content observed in size fraction  $<0.49\ \mu\text{m}$  from UT suggest photochemical formation of secondary organic compounds (mainly in the accumulation mode ( $<0.1\ \mu\text{m}$ ) with oxygen-containing functional groups that increase solubility in water [55].

The content of carbonaceous species in size fraction  $<0.49\ \mu\text{m}$  is illustrated in Figure 3b. In both seasons, EC was evidently higher at the UT site as a result of higher traffic emissions in close proximity. OC was also relatively higher at the UT site compared to UB. The water-soluble fraction of OC (WSOC/OC) exhibited large seasonal variation at UT being largest (44%) in summer and lowest (16%) in winter, whereas it was stable (38%) in all seasons at UB.

### 3.3. Trace Organic Compounds

The volumetric concentrations of trace organic compounds determined in PM from UT and UB have been reported in [40]. The size distribution and the spatiotemporal variation of their content are discussed below.

#### 3.3.1. PAHs

The size distributions of the contents of the 12 PAHs ( $\Sigma_{12}\text{PAHs}$ ), and the class-1 carcinogen B[a]P are shown in Figure 4a,b. The highest  $\Sigma_{12}\text{PAH}$  content across sites and seasons was associated with the  $0.49\text{--}0.97\ \mu\text{m}$  particle size fraction followed by the  $<0.49\ \mu\text{m}$  fraction thus suggesting origin from traffic emissions. It is also worth noting the relatively high  $\Sigma_{12}\text{PAH}$  content of the wintertime coarse fraction ( $>3\ \mu\text{m}$ ) from the UB site that should be probably attributed to the intensive wood burning for residential heating in this area [40,56]. B[a]P revealed similar size distribution pattern with  $\Sigma_{12}\text{PAH}$  exhibiting its largest content in wintertime particle size fractions  $0.49\text{--}0.97\ \mu\text{m}$  from UT, and  $0.97\text{--}3\ \mu\text{m}$  from UB.

An intra-site difference was apparent, particularly in the warm period, with all particle size fractions exhibiting higher PAH content at the UT site due to closer proximity to dense vehicular traffic. In contrast, the wintertime coarse fraction from the UB site exhibited higher PAH content compared with the corresponding fraction from the UT site due to wood burning emissions.

PM fractions from the UT site exhibited only slightly higher  $\Sigma_{12}\text{PAH}$  content in wintertime, while the coarse fraction appeared to be more enriched with PAHs in the warm period (cold/warm ratios 1.6, 1.3, 1.5, and 0.6, respectively). In contrast, PM fractions from the UB site exhibited  $\Sigma_{12}\text{PAH}$  content significantly higher in winter with cold/warm ratios of the 6.3, 3.0, 6.5, and 11.5, respectively. Higher PAH content in the cold period is a combined result of prominent emissions from primary sources (i.e., domestic heating and vehicular traffic), and the increased sorption of the most volatile PAHs on particles. Conversely, lower PAH content during the warm period is due to decreased emissions from heating sources, to meteorological conditions that favor the gas-phase partition of PAHs, and the photodegradation of the most reactive PAH species triggered by solar radiation and chemical oxidations by atmospheric oxidants such as ozone and radicals [57].

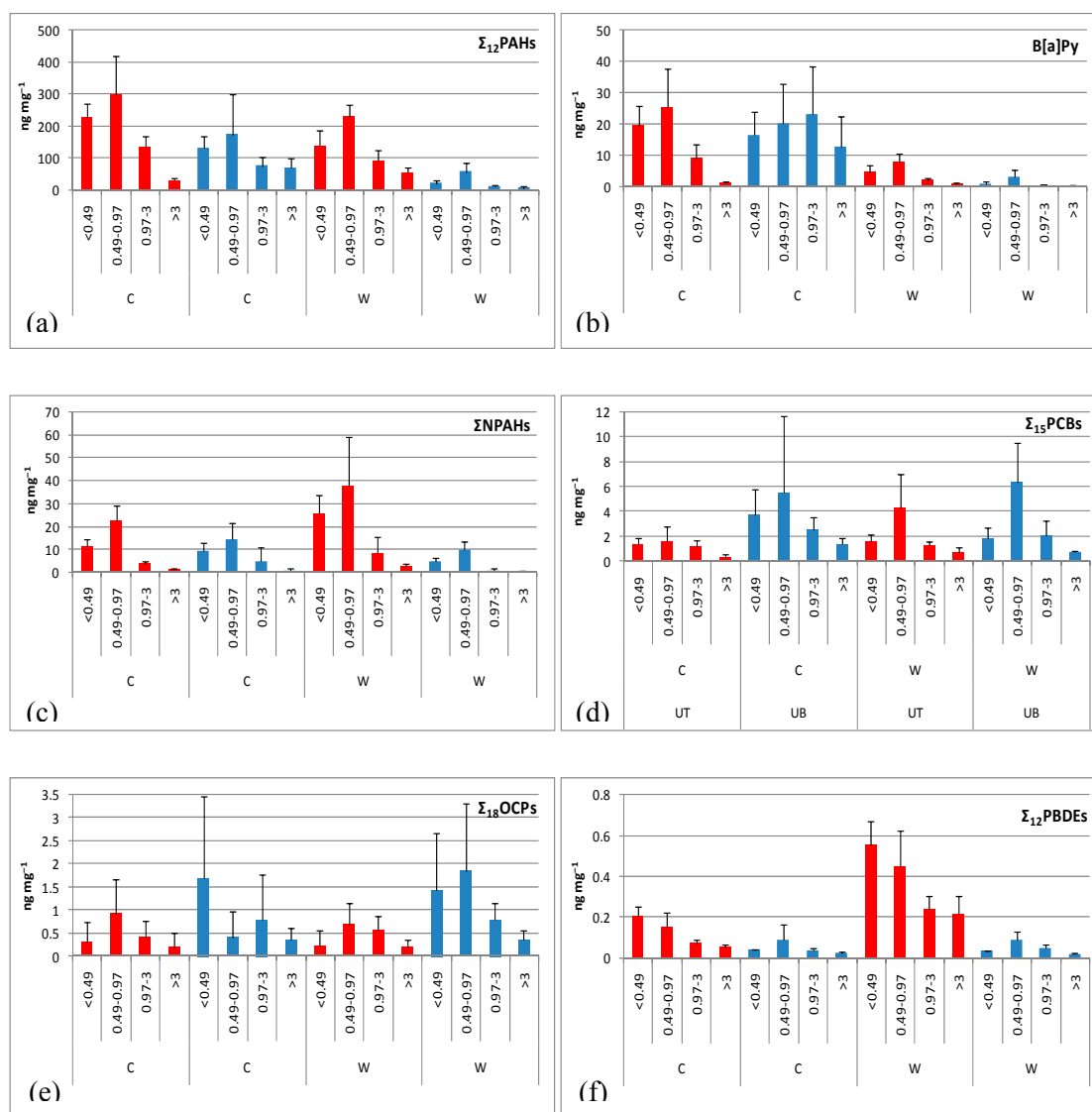


**Figure 4.** Mean  $\pm$  SD of the content of trace organic compounds in size-segregated PM; (a–f) are  $\Sigma_{12}$ PAHs, B[a]Py,  $\Sigma$ NPAHs,  $\Sigma_{15}$ PCBs,  $\Sigma_{18}$ OCPs,  $\Sigma_{12}$ PBDEs, respectively.

### 3.3.2. Nitro-PAHs

Similarly to  $\Sigma_{12}$ PAHs, the highest  $\Sigma$ NPAH contents across sites and seasons were associated with the 0.49–0.97  $\mu\text{m}$  particle size fraction, whereas the lowest with the coarse fraction (Figure 4c). An intra-site difference was apparent, particularly in the warm period, with all particle size fractions exhibiting higher  $\Sigma$ NPAH content at UT. This could be attributed to the close proximity of this site to dense vehicular traffic considering that the major primary source of NPAHs is PAHs nitration during diesel and/or gasoline combustion.

The  $\Sigma$ NPAH content exhibited contrasting seasonal pattern at the two sites. At the UT site, all size fractions exhibited higher content in summer suggesting additional secondary formation of NPAHs under increased solar radiation by either gas-phase reactions with hydroxyl and nitrate radicals followed by reaction with nitrogen dioxide, or heterogeneous reactions of particulate PAHs with nitrating agents [58]. In contrast, at the UB site, all size fractions exhibited higher  $\Sigma$ NPAH content in winter attributable to domestic heating (wood burning is a primary source of NPAHs, although by far less important than diesel), and seasonality in gas-particle partitioning.

### 3.3.3. PCBs and OCPs

The highest content of total PCBs ( $\Sigma_{15}$ PCBs) was associated with the 0.49–0.97  $\mu\text{m}$  particle size fraction, whereas the lowest with the coarse fraction (Figure 4d). Interestingly enough, all PM size fractions exhibited significantly higher content at the UB site, particularly in the cold period, although the intra-site differences were less apparent in the warm period.

The total OCPs content exhibited similar size distribution, intra-site and seasonal patterns with PCBs (Figure 4e). The higher OCPs content at the UB site, particularly in the warm period, might be attributed to the close vicinity of this site to forest and agricultural areas [40].

### 3.3.4. PBDEs

$\Sigma_{12}$ PBDE content at UT exhibited a clear enrichment in the smallest particle fraction <0.49  $\mu\text{m}$ , whereas at UB the highest content was shifted to relatively larger sizes (0.49–0.97  $\mu\text{m}$ ) (Figure 4f). All PM fractions appeared to be more enriched with PBDEs at UT in comparison to UB, particularly in the warm period. This can be explained considering that emissions of PBDEs are usually higher in urban centers and densely populated residential areas mainly through the outgassing of contaminated air from homes, offices and cars [40]. The  $\Sigma_{12}$ PBDE content exhibited significant seasonality only at UT with values higher in the warm period (cold/warm ratios 0.4, 0.3, 0.3 and 0.2 for the four particle fractions).

### 3.3.5. Polar Organic Marker Compounds

The contents of DCAs and levoglucosan in size fraction <0.49  $\mu\text{m}$  are shown in Figure 5.

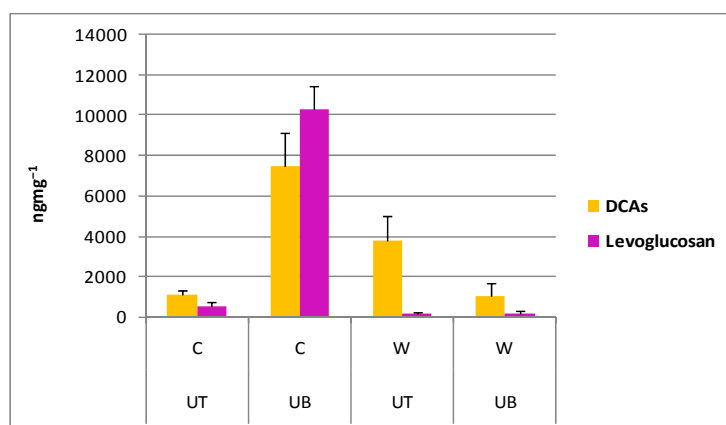


**Figure 5.** Mean  $\pm$  SD of the content of polar organic marker compounds in the <0.49  $\mu\text{m}$  particle fraction (UT: urban traffic site; UB: urban background site; C: cold period; W: warm period).

Levoglucosan, commonly considered as a suitable organic tracer for biomass burning [59], exhibited its highest content during wintertime at UB. DCAs also exhibited their highest content during wintertime at UB that is attributed to preferential origin related to biomass combustion [59]. Noticeable DCAs content was also found in summertime  $\text{PM}_{0.49}$  at UT, suggesting possible secondary formation through photo-chemical reactions from volatile precursors emitted from vehicles [60].

### 3.4. Correlations between DTT Activity and Organic Aerosol Components

Usually, the identification of specific PM components as contributors to DTT activity is based on the correlation of DTT activity with PM composition. Nevertheless, correlations do not show causation, especially since PM constituents often highly covariate [31], while the small sample size (often  $n < 30$ ) limits the statistical significance of the inferred associations [36].

The Spearman's rank or the Pearson correlation coefficients between the DTT activity and the mass fractions of organic chemical components determined in the various size fractions of PM in the present study are provided in Tables 2 and 3 for the UT and the UB site, respectively.

When the total data sets ( $n = 40$ ) were considered, correlations between DTT activity and WSOC were insignificant at both sites. Nevertheless, statistically significant correlation (0.449,  $p < 0.05$ ) was obtained for wintertime samples from UT suggesting that there is a wintertime WSOC source at this site—other than secondary photochemical formation—that contributes to the DTT activity in winter.

At both sites, DTT activity exhibited only few positive correlations with PAHs and NPAHs. This could be explained by the fact that PAHs are not redox-active and their correlation with DTT loss is due to a correlation between PAHs and quinones [12]. It is worth noting that the solvent-extractable DTT activity of PM from Thessaloniki was previously found to be significantly correlated with PAHs (Fl, B[a]Py, B[e]Py, B[b]Fl, IPy, B[ghi]Pe), and NPAHs as well (1-NPy, 2-NFl) [23,24].

Interestingly, DTT activity at both sites appeared to significantly correlate with non-polar organic compounds, such as (e.g., BDEs-15, -28, -153, -154, *o,p'*-DDT, *o,p'*-DDE, dieldrin,  $\Sigma$ OCPs, PCBs-105, -180, -77, and  $\Sigma_{15}$ PCBs at the UT site, as well as BDEs -15, -17, -28, -154, -153,  $\Sigma_{12}$ PBDEs, and  $\Sigma_{15}$ PCBs at the UB site). It is not known if these strongly hydrophobic compounds are active in the DTT assay, or simply correlate with other water-soluble redox-active species. Correlation with non-polar organic compounds, such as n-alkanes (C<sub>14</sub>-C<sub>32</sub>), isoprenoids (pristane, phytane), and OCPs (a-HCH, quintozene, *p-p'*-DDT) was also found for the solvent-extractable DTT activity of PM from Thessaloniki [23,24].

Concerning the <0.49  $\mu\text{m}$  fraction, at the UB site, DTT activity was correlated with both OC and EC. The latter might be attributed to the fact that EC correlates highly with PAHs, DCAs, and levoglucosan (0.782, 0.891, and 0.794,  $p < 0.01$ ) which suggests that it is contributed by biomass burning rather than vehicle emissions. Similar findings (i.e., correlation of EC with DTT activity and biomass burning markers such as brown carbon and K) have been reported in [36]. DTT activity at the UB site exhibited high correlations with most DCAs, excepting glutaric and  $\alpha$ -ketoglutaric, particularly in wintertime, implying impact from biomass combustion emissions [59]. This is further confirmed by the strong correlation found at the UB site between DTT activity and levoglucosan which is in line with previous findings that residential wood burning is the major contributor to the DTT activity of PM<sub>0.49</sub> at this site [28]. At the UT site, DTT activity was not correlated with OC, while it was significantly correlated with the wintertime EC only (0.894,  $p < 0.05$ ). In contrast to the UB site, DTT activity was significantly correlated with all DCAs, particularly in summertime, suggesting impact from SOC sources [40].

Several studies have reported strong correlations between DTT activity and organic PM components either the bulk groups of organic species, i.e., OC and WSOC [12,15,19,29,36,52,61], or specific organic compounds such as PAHs [14,25,27,49], quinones [62], levoglucosan [12,14,15,18,25,27,28,50,61], and other biomass burning markers [36]. High correlations with hopanes, in addition to OC and PAHs, have also been reported in some studies [12,15,26,42,61,63], while Shirmohammadi et al. [27] found high correlations with hopanes, n-alkanes, and organic acids (phthalic, succinic, and glutaric). Differently from above, in Perrone et al. [44], the methanol-soluble DTT activity of PM exhibited negative correlations with most chemical constituents including n-alkanes, being positively correlated mainly with global radiation, which was considered as a proxy for secondary oxidizing organics. Secondary organic compounds have higher DTT activity than their parent gases and primary particles [15,32]. Chirizzi et al. [29] found relatively higher correlation coefficients for secondary organic carbon (SOC) compared with primary organic carbon (POC).

In general, findings from studies may vary widely with regard to the most DTT-active PM fraction and relation to PM composition. Moreover, the low water-solubility of primary organic compounds, which are mostly hydrophobic, could influence the correlations with the water-soluble DTT activity.

**Table 2.** Spearman and Pearson (italicized values) correlation coefficients between the mass-normalized DTT activity and the content of organic chemical components in PM from the urban traffic site (UT).

|                                     | <i>n</i> = 40 | <i>n</i> = 40                                      | <i>n</i> = 40                                  | <i>n</i> = 40                                     | <i>n</i> = 10               |
|-------------------------------------|---------------|--|--|---|-----------------------------|
| WSOC                                | 0.127         | PCB-28(+31) 0.300                                  | $\alpha$ -HCH 0.217                            | BDE-15 0.768 **                                   | Maleic 0.797 **             |
| Ph                                  | 0.159         | PCB-52 0.284                                       | HCB −0.025                                     | BDE-17 0.076                                      | Succinic 0.810 **           |
| An                                  | 0.231         | PCB-101 0.264                                      | $\gamma$ -HCH 0.145                            | BDE-28 0.595 **                                   | Glutaric 0.898 **           |
| Fl                                  | 0.038         | PCB-77 0.387 *                                     | $\beta$ -HCH 0.081                             | BDE-49(+71) 0.250                                 | Malic 0.667 *               |
| Py                                  | 0.072         | PCB-118 0.008                                      | heptachlor 0.155                               | BDE-47 0.027                                      | Salicylic 0.748 *           |
| B[a]An                              | 0.100         | PCB-153 0.230                                      | aldrin −0.090                                  | BDE-66 0.193                                      | a-ketoglutaric 0.835 **     |
| Chry                                | 0.182         | PCB-105 0.460 **                                   | isobenzan −0.301                               | BDE-100 0.238                                     | Phthalic 0.736 *            |
| B[b]Fl                              | 0.302         | PCB-138 0.030                                      | isodrin 0.120                                  | BDE-99 −0.040                                     | <b>DCAs</b> <b>0.847 **</b> |
| B[k]Fl                              | 0.068         | PCB-126 0.122                                      | cis-heptachlor 0.262                           | BDE-154 0.452 **                                  | Levogluconan −0.767 **      |
| B[a]Py                              | 0.027         | PCB-128 −0.380 *                                   | <i>o,p'</i> -DDE 0.370 *                       | BDE-153 0.442 **                                  |                             |
| I[1,2,3-cd]Py                       | 0.385 *       | PCB-156 0.074                                      | endrin −0.053                                  | BDE-183 −0.751 **                                 |                             |
| dB[a,h]An                           | 0.342 *       | PCB-180 0.410 **                                   | <i>p,p'</i> -DDE 0.107                         | <b><math>\Sigma_{12}</math>PBDEs</b> <b>0.040</b> | OC −0.250                   |
| B[ghi]Pe                            | 0.134         | PCB-169 −0.069                                     | <i>o,p'</i> -DDD 0.196                         |   | EC 0.461                    |
| <b><math>\Sigma_{12}</math>PAHs</b> | <b>0.213</b>  | PCB-170 0.084                                      | dieldrin 0.400 *                               |   |                             |
|                                     |               | <b><math>\Sigma_{15}</math>PCBs</b> <b>0.344 *</b> | $\beta$ -endosulfan −0.091                     |   |                             |
| 1-NNp                               | 0.281         |  | <i>p,p'</i> -DDD 0.172                         |   |                             |
| 2-NNp                               | 0.101         |  | <i>o,p'</i> -DDT 0.497 **                      |   |                             |
| 5-NAce                              | 0.439 **      |  | <i>p,p'</i> -DDT 0.076                         |   |                             |
| 3-NBPHE                             | 0.116         |  | <b><math>\Sigma</math>OCPs</b> <b>0.507 **</b> |   |                             |
| 4-NBPHE                             | 0.213         |  |  |   |                             |
| 3-NFl                               | 0.156         |  |  |   |                             |
| 1-NPy                               | 0.168         |  |  |   |                             |
| <b><math>\Sigma</math>NPAHs</b>     | <b>0.173</b>  |  |  |   |                             |

\*\* Correlation is significant at the 0.01 level (two-tailed); \* Correlation is significant at the 0.05 level (two-tailed).

**Table 3.** Spearman and Pearson (italicized values) correlation coefficients between the mass-normalized DTT activity and the content of organic chemical components in PM from the urban background site (UB).

| <i>n</i> = 40             |              | <i>n</i> = 40             |                | <i>n</i> = 40    |               | <i>n</i> = 40              |                | <i>n</i> = 10  |                 |
|---------------------------|--------------|---------------------------|----------------|------------------|---------------|----------------------------|----------------|----------------|-----------------|
| WSOC                      | 0.072        | PCB-28(+31)               | −0.176         | α-HCH            | 0.186         | BDE-15                     | 0.611 **       | Maleic         | 0.824 **        |
|                           |              | PCB-52                    | 0.231          | HCb              | −0.107        | BDE-17                     | 0.472 **       | Succinic       | 0.676 *         |
| Ph                        | 0.038        | PCB-101                   | 0.182          | γ-HCH            | 0.129         | BDE-28                     | 0.353 *        | Glutaric       | 0.515           |
| An                        | −0.107       | PCB-77                    | 0.068          | β-HCH            | −0.117        | BDE-49 + 71                | 0.182          | Malic          | 0.860 **        |
| Fl                        | 0.130        | PCB-118                   | −0.048         | heptachlor       | 0.034         | BDE-47                     | 0.298          | Salicylic      | 0.813 **        |
| Py                        | 0.134        | PCB-153                   | −0.024         | aldrin           | −0.092        | BDE-66                     | −0.070         | a-ketoglutaric | 0.523           |
| B[a]An                    | 0.325 *      | PCB-105                   | −0.021         | isobenzan        | 0.015         | BDE-100                    | 0.020          | Phthalic       | 0.795 **        |
| Chry                      | 0.137        | PCB-138                   | 0.037          | isodrin          | −0.435 **     | BDE-99                     | 0.124          | <b>DCAs</b>    | <b>0.800 **</b> |
| B[b]Fl                    | −0.235       | PCB-126                   | 0.095          | cis-heptachlor   | 0.006         | BDE-154                    | 0.507 **       | Levogluconan   | 0.732 *         |
| B[k]Fl                    | 0.088        | PCB-128                   | 0.212          | <i>o,p'</i> -DDE | 0.125         | BDE-153                    | 0.549 **       |                |                 |
| B[a]Py                    | 0.224        | PCB-156                   | 0.148          | endrin           | 0.009         | BDE-183                    | −0.058         |                |                 |
| I[1,2,3-cd]Py             | 0.294        | PCB-180                   | −0.202         | <i>p,p'</i> -DDE | −0.384 *      | <b>Σ<sub>12</sub>PBDEs</b> | <b>0.371 *</b> | OC             | 0.845 **        |
| dB[a,h]An                 | 0.008        | PCB-169                   | 0.034          | <i>o,p'</i> -DDD | −0.454 **     |                            |                | EC             | 0.693 *         |
| B[ghi]Pe                  | 0.260        | PCB-170                   | −0.219         | dieldrin         | −0.055        |                            |                |                |                 |
| <b>Σ<sub>12</sub>PAHs</b> | <b>0.176</b> | <b>Σ<sub>15</sub>PCBs</b> | <b>0.347 *</b> | β-endosulfan     | −0.088        |                            |                |                |                 |
|                           |              |                           |                | <i>p,p'</i> -DDD | −0.043        |                            |                |                |                 |
| 1-NNp                     | −0.248       |                           |                | <i>o,p'</i> -DDT | −0.117        |                            |                |                |                 |
| 2-NNp                     | −0.350 *     |                           |                | <i>p,p'</i> -DDT | −0.015        |                            |                |                |                 |
| 5-NAce                    | −0.255       |                           |                | <b>ΣOCPs</b>     | <b>−0.109</b> |                            |                |                |                 |
| 3-NBPHE                   | −0.051       |                           |                |                  |               |                            |                |                |                 |
| 4-NBPHE                   | 0.154        |                           |                |                  |               |                            |                |                |                 |
| 3-NFl                     | −0.052       |                           |                |                  |               |                            |                |                |                 |
| 1-NPy                     | 0.116        |                           |                |                  |               |                            |                |                |                 |
| <b>ΣNPAHs</b>             | <b>0.052</b> |                           |                |                  |               |                            |                |                |                 |

\*\* Correlation is significant at the 0.01 level (two-tailed); \* Correlation is significant at the 0.05 level (two-tailed).

#### 4. Conclusions

Water-soluble DTT activity was measured in size-segregated PM samples from an urban traffic (UT) and an urban background (UB) site during the cold and the warm season. At both sites, DTT activity maximized in the 0.49–0.97  $\mu\text{m}$  particle fraction decreasing onwards almost linearly with increasing particle size. The <0.49  $\mu\text{m}$  particle fraction exhibited the lowest DTT activity implying that particles of the quasi-UFP mode, although accounting for more than 50% of the total PM mass, are less enriched with DTT-active substances in comparison to larger particles. DTT activity exhibited different seasonal variation in the different particle fractions. Overall, excepting summertime particle fractions <0.49  $\mu\text{m}$  and >3  $\mu\text{m}$ , that exhibited higher DTT activity at the UT site, thus suggesting the dominant contribution of traffic-related emissions, in all other PM samples, DTT activity was higher at the UB site that is characterized by increased biomass burning.

DTT activity was insignificantly correlated with WSOC at both sites, while it exhibited only few correlations with PAHs. In contrast, significant correlations were observed with non-polar organic compounds such as PCBs, OCPs and PBDEs, that need further investigation since these chemical classes are highly hydrophobic. In addition, in the <0.49  $\mu\text{m}$  fraction, DTT activity was highly correlated with EC at both sites and with OC at the UB site underscoring the great impact of vehicle tailpipe emissions and other combustion sources on the oxidative potential of PM in this size range. Other significant correlations in the <0.49  $\mu\text{m}$  fraction were with polar organic compounds such as DCAs, particularly in summer at the UT site and in winter at the UB site, indicative of the impacts of SOC and biomass burning emissions, respectively. The impact of biomass burning emissions on the oxidative potential of PM at the UT site was further confirmed by the strong correlation between DTT activity and levoglucosan, the most suitable tracer of biomass burning. Conclusively, results of this study indicated association of the water-soluble DTT activity of urban PM with various polar, and therefore more hydrophilic, organic compounds of secondary or primary origin. However, further research is essential to outline the role of the hydrophobic organic PM species in the oxidative activity of water-soluble PM.

**Acknowledgments:** The results presented and discussed in this article were obtained through the research project THALES “Bioactivity of airborne particulates in relation with their size, morphology and chemical composition” (MIS 377304), which was co-financed by the European Social Fund (ESF) and the Greek Ministry of Education.

**Conflicts of Interest:** The author declares no conflict of interest.

#### References

1. Brunekreef, B.; Holgate, S.T. Air pollution and health. *Lancet* **2002**, *360*, 1233–1242. [[CrossRef](#)]
2. Pope, C.A.; Burnett, R.T.; Thun, M.; Calle, E.E.; Krewski, D.; Ito, K.; Thurston, G.D. Lung cancer, cardiopulmonary mortality, and long-term exposure to fine particulate air pollution. *J. Am. Med. Assoc.* **2002**, *287*, 1132–1141. [[CrossRef](#)]
3. Delfino, R.J.; Staimer, N.; Tjoa, T.; Arhami, M.; Polidori, A.; Gillen, D.L.; Kleinman, M.T.; Schauer, J.J.; Sioutas, C. Association of Biomarkers of Systemic Inflammation with Organic Components and Source Tracers in Quasi-Ultrafine Particles. *Environ. Health Perspect.* **2010**, *118*, 756–762. [[CrossRef](#)] [[PubMed](#)]
4. Kelly, F.J.; Fussell, J.C. Air pollution and public health: Emerging hazards and improved understanding of risk. *Environ. Geochem. Health* **2015**, *37*, 631–649. [[CrossRef](#)] [[PubMed](#)]
5. Nel, A. Air pollution related illness: Effects of particles. *Science* **2005**, *308*, 804–806. [[CrossRef](#)] [[PubMed](#)]
6. Borm, P.J.A.; Kelly, F.; Künzli, N.; Schins, R.P.F.; Donaldson, K. Oxidant generation by particulate matter: From biologically effective dose to a promising, novel metric. *Occup. Environ. Med.* **2007**, *64*, 73–74. [[CrossRef](#)] [[PubMed](#)]
7. Janssen, N.A.H.; Strak, M.; Yang, A.; Hellack, B.; Kelly, F.; Kuhlbusch, T.; Harrison, R.; Brunekreef, B.; Cassee, F.; Steenhof, M.; et al. Associations between three specific a-cellular measures of the oxidative potential of particulate matter and markers of acute airway and nasal inflammation in healthy volunteers. *Occup. Environ. Med.* **2015**, *72*, 49–56. [[CrossRef](#)] [[PubMed](#)]

8. Boogaard, H.; Janssen, N.A.; Fischer, P.H.; Kos, G.P.; Weijers, E.P.; Cassee, F.R.; van der Zee, S.C.; de Hartog, J.J.; Brunekreef, B.; Hoek, G. Contrasts in Oxidative Potential and Other PM Characteristics Collected Near Major Streets and Background Locations. *Environ. Health Perspect.* **2012**, *120*, 185–191. [[CrossRef](#)] [[PubMed](#)]
9. Fang, T.; Verma, V.; Bates, J.T.; Abrams, J.; Klein, M.; Strickland, M.J.; Sarnat, S.E.; Chang, H.H.; Mulholland, J.A.; Tolbert, P.E.; et al. Oxidative potential of ambient water-soluble PM<sub>2.5</sub> in the southeastern United States: Contrasts in sources and health associations between ascorbic acid (AA) and dithiothreitol (DTT) assays. *Atmos. Chem. Phys.* **2016**, *16*, 3865–3879. [[CrossRef](#)]
10. Ayres, J.G.; Borm, P.; Cassee, F.R.; Castranova, V.; Donaldson, K.; Ghio, A.; Harrison, R.M.; Hider, R.; Kelly, F.; Kooter, I.M.; et al. Evaluating the toxicity of airborne particulate matter and nanoparticles by measuring oxidative stress potential—A workshop report and consensus statement. *Inhal. Toxicol.* **2008**, *20*, 75–99. [[CrossRef](#)] [[PubMed](#)]
11. Venkatachari, P.; Hopke, P.; Grover, B.D.; Eatough, D.J. Measurement of particle-bound reactive species in Rubidoux aerosols. *J. Atmos. Chem.* **2005**, *50*, 49–58. [[CrossRef](#)]
12. Cho, A.K.; Sioutas, C.; Miguel, A.H.; Kumagai, Y.; Schmitz, D.A.; Singh, M.; Eiguren-Fernandez, A.; Froines, J.R. Redox activity of airborne particulate matter at different sites in the Los Angeles Basin. *Environ. Res.* **2005**, *99*, 40–47. [[CrossRef](#)] [[PubMed](#)]
13. Kumagai, Y.; Koide, S.; Taguchi, K.; Endo, A.; Nakai, Y.; Yoshikawa, T.; Shimojo, N. Oxidation of proximal protein sulfhydryls by phenanthraquinone, a component of diesel exhaust particles. *Chem. Res. Toxicol.* **2002**, *15*, 483–489. [[CrossRef](#)] [[PubMed](#)]
14. Li, N.; Sioutas, C.; Cho, A.; Schmitz, D.; Misra, C.; Sempf, J.; Wang, M.; Oberley, T.; Froines, J.; Nel, A. Ultrafine particulate pollutants induce oxidative stress and mitochondrial damage. *Environ. Health Perspect.* **2003**, *111*, 455–460. [[CrossRef](#)]
15. Verma, V.; Ning, Z.; Cho, A.K.; Schauer, J.J.; Shafer, M.M.; Sioutas, C. Redox activity of urban quasi-ultrafine particles from primary and secondary sources. *Atmos. Environ.* **2009**, *43*, 6360–6368. [[CrossRef](#)]
16. Li, N.; Wang, M.; Bramble, L.A.; Schmitz, D.A.; Schauer, J.J.; Sioutas, C.; Harkema, J.R.; Nel, A.E. The Adjuvant Effect of Ambient Particulate Matter Is Closely Reflected by the Particulate Oxidant Potential. *Environ. Health Persp.* **2009**, *117*, 1116–1123. [[CrossRef](#)] [[PubMed](#)]
17. Steenhof, M.; Gosens, I.; Strak, M.; Godri, K.J.; Hoek, G.; Cassee, F.R.; Mudway, I.S.; Kelly, F.J.; Harrison, R.M.; Lebret, E.; et al. In vitro toxicity of particulate matter (PM) collected at different sites in the Netherlands is associated with PM composition, size fraction and oxidative potential—The RAPTES project. *Part. Fibre Toxicol.* **2011**, *8*, 26. [[CrossRef](#)] [[PubMed](#)]
18. Velali, E.; Papachristou, E.; Pantazaki, A.; Choli-Papadopoulou, T.; Planou, S.; Kouras, A.; Manoli, E.; Besis, A.; Voutsas, D.; Samara, C. Redox activity and in vitro bioactivity of the water-soluble fraction of urban particulate matter in relation to particle size and chemical composition. *Environ. Pollut.* **2016**, *208*, 774–786. [[CrossRef](#)] [[PubMed](#)]
19. Verma, V.; Rico-Martinez, R.; Kotra, N.; King, L.; Liu, J.; Snell, T.W.; Weber, R.J. Contribution of water-soluble and insoluble components and their Hydrophobic/Hydrophilic subfractions to the reactive oxygen species-generating potential of Fine ambient aerosols. *Environ. Sci. Technol.* **2012**, *46*, 11384–11392. [[CrossRef](#)] [[PubMed](#)]
20. Verma, V.; Fang, T.; Xu, L.; Peltier, R.E.; Russell, A.G.; Ng, N.L.; Weber, R.J. Organic aerosols associated with the generation of reactive oxygen species (ROS) by water-soluble PM<sub>2.5</sub>. *Environ. Sci. Technol.* **2015**, *49*, 4646–4656. [[CrossRef](#)] [[PubMed](#)]
21. Rattanavaraha, W.; Rosen, E.; Zhang, H.; Li, Q.; Pantong, K.; Kamens, R.M. The reactive oxidant potential of different types of aged atmospheric particles: An outdoor chamber study. *Atmos. Environ.* **2011**, *45*, 3848–3855. [[CrossRef](#)]
22. Yang, A.; Jedynska, A.; Hellack, B.; Kooter, I.; Hoek, G.; Brunekreef, B.; Kuhlbusch, T.A.J.; Cassee, F.R.; Janssen, N.A.H. Measurement of the oxidative potential of PM<sub>2.5</sub> and its constituents: The effect of extraction solvent and filter type. *Atmos. Environ.* **2014**, *83*, 35–42. [[CrossRef](#)]
23. Chrysikou, L.P.; Samara, C. Redox activity and organic chemical composition of size segregated PM in Thessaloniki, northern Greece. In Proceedings of the 11th International Conference on Environmental Science and Technology (CEST2009), Chania, Crete, Greece, 3–5 September 2009.

24. Samara, C.; Chrysikou, L. Mutagenicity and redox activity of size segregated airborne particulate matter in Thessaloniki, Northern Greece, in relation to aerosol chemical composition. *Front. Pharmacol.* **2010**. [[CrossRef](#)]
25. Ntziachristos, L.; Froines, J.R.; Cho, A.K.; Sioutas, C. Relationship between redox activity and chemical speciation of size-fractionated particulate matter. *Part. Fibre Toxicol.* **2007**, *4*, 5. [[CrossRef](#)] [[PubMed](#)]
26. Saffari, A.; Daher, N.; Shafer, M.M.; Schauer, J.J.; Sioutas, C. Seasonal and spatial variation in dithiothreitol (DTT) activity of quasi-ultrafine particles in the Los Angeles Basin and its association with chemical species. *J. Environ. Sci. Health A Tox. Hazard Subst. Environ. Eng.* **2014**, *49*, 441–451. [[CrossRef](#)] [[PubMed](#)]
27. Shirmohammadi, F.; Hasheminassab, S.; Wang, D.; Schauer, J.J.; Shafer, M.; Delfino, R.J.; Sioutas, C. The relative importance of tailpipe and nontailpipe emissions on the oxidative potential of ambient particles in Los Angeles, CA. *Faraday Discuss.* **2016**, *189*, 361–380. [[CrossRef](#)] [[PubMed](#)]
28. Argyropoulos, G.; Besis, A.; Voutsas, D.; Samara, C.; Sowlat, M.H.; Hasheminassab, S.; Sioutas, C. Source apportionment of the redox activity of urban quasi-ultrafine particles (PM<sub>0.49</sub>) in Thessaloniki following the increased biomass burning due to the economic crisis in Greece. *Sci. Total Environ.* **2016**, *568*, 124–136. [[CrossRef](#)] [[PubMed](#)]
29. Chirizzi, D.; Cesari, D.; Guascito, M.R.; Dinoi, A.; Giotta, L.; Donato, A.; Contini, D. Influence of Saharan dust outbreaks and carbon content on oxidative potential of water-soluble fractions of PM<sub>2.5</sub> and PM<sub>10</sub>. *Atmos. Environ.* **2017**, *163*, 1–8. [[CrossRef](#)]
30. Verma, V.; Pakbin, P.; Cheung, K.L.; Cho, A.K.; Schauer, J.J.; Shafer, M.M.; Kleinman, M.T.; Sioutas, C. Physicochemical and oxidative characteristics of semi-volatile components of quasi ultrafine particles in an urban atmosphere. *Atmos. Environ.* **2011**, *45*, 1025–1033. [[CrossRef](#)]
31. Charrier, J.G.; Anastasio, C. On dithiothreitol (DTT) as a measure of oxidative potential for ambient particles: Evidence for the importance of soluble transition metals. *Atmos. Chem. Phys. Discuss.* **2012**, *12*, 8533–8546. [[CrossRef](#)] [[PubMed](#)]
32. Li, Q.F.; Wyatt, A.; Kamens, R.M. Oxidant generation and toxicity enhancement of aged-diesel exhaust. *Atmos. Environ.* **2009**, *43*, 1037–1042. [[CrossRef](#)]
33. Lin, P.; Yu, J.Z. Generation of reactive oxygen species mediated by humic-like substances in atmospheric aerosols. *Environ. Sci. Technol.* **2011**, *45*, 10362–10368. [[CrossRef](#)] [[PubMed](#)]
34. Fang, T.; Guo, H.; Zeng, L.; Verma, V.; Nenes, A.; Weber, R.J. Highly Acidic Ambient Particles, Soluble Metals, and Oxidative Potential: A Link between Sulfate and Aerosol Toxicity. *Environ. Sci. Technol.* **2017**, *51*, 2611–2620. [[CrossRef](#)] [[PubMed](#)]
35. Bates, J.T.; Weber, R.J.; Abrams, J.; Verma, V.; Fang, T.; Klein, M.; Strickland, M.J.; Sarnat, S.E.; Chang, H.H.; Mulholland, J.A.; et al. Reactive oxygen species generation linked to sources of atmospheric particulate matter and cardiorespiratory effects. *Environ. Sci. Technol.* **2015**, *49*, 13605–13612. [[CrossRef](#)] [[PubMed](#)]
36. Verma, V.; Fang, T.; Guo, H.; King, L.; Bates, J.T.; Peltier, R.E.; Edgerton, E.; Russell, A.G.; Weber, R.J. Reactive oxygen species associated with water-soluble PM<sub>2.5</sub> in the southeastern United States: spatiotemporal trends and source apportionment. *Atmos. Chem. Phys.* **2014**, *14*, 12915–12930. [[CrossRef](#)]
37. Besis, A.; Botsaropoulou, E.; Voutsas, D.; Samara, C. Particle-size distribution of polybrominated diphenyl ethers (PBDEs) in the urban agglomeration of Thessaloniki, northern Greece. *Atmos. Environ.* **2015**, *104*, 176–185. [[CrossRef](#)]
38. Planou, S.; Voutsas, D.; Samara, C. Water soluble organic carbon (WSOC) content and redox activity of size-segregated PM in Thessaloniki, Northern Greece. In Proceedings of the 14th International Conference on Environmental Science and Technology (CEST2015), Rhodes, Greece, 3–5 September 2015.
39. Samara, C.; Kantiranis, N.; Kollias, P.; Planou, S.; Kouras, A.; Besis, A.; Manoli, E.; Voutsas, D. Spatial and seasonal variations of the chemical, mineralogical and morphological features of quasi-ultrafine particles (PM<sub>0.49</sub>) at urban sites. *Sci. Total Environ.* **2016**, *553*, 392–403. [[CrossRef](#)] [[PubMed](#)]
40. Besis, A.; Tsolakidou, A.; Balla, D.; Samara, C.; Voutsas, D.; Pantazaki, A.; Choli-Papadopoulou, T.; Lialiaris, T.S. Toxic organic substances and marker compounds in size-segregated urban particulate matter—Implications for involvement in the in vitro bioactivity of the extractable organic matter. *Environ. Pollut.* **2017**, *230*, 758–774. [[CrossRef](#)] [[PubMed](#)]
41. Voutsas, D.; Besis, A.; Tsolakidou, A.; Balla, D.; Samara, C. Particle size distribution of persistent organic pollutants and polar organic marker compounds at traffic and urban background sites. In Proceedings of the 15th EuCheMS International Conference on Chemistry and the Environment (ICCE2015), Leipzig, Germany, 20–24 September 2015; p. 379.

42. Samara, C.; Kouras, A.; Kaidoglou, K.; Emmanouil-Nikoloussi, E.-N.; Simou, C.; Bousnaki, M.; Kelessis, A. Ultrastructural alterations in the mouse lung caused by real-life ambient PM10 at urban traffic sites. *Sci. Total Environ.* **2015**, *532*, 327–336. [[CrossRef](#)] [[PubMed](#)]
43. Janssen, N.A.H.; Yang, A.; Strak, M.; Steenhof, M.; Hellack, B.; Gerlofs-Nijland, M.E.; Kuhlbusch, T.; Kelly, F.; Harrison, R.; Brunekreef, B.; et al. Oxidative potential of particulate matter collected at sites with different source characteristics. *Sci. Total Environ.* **2014**, *472*, 572–581. [[CrossRef](#)] [[PubMed](#)]
44. Perrone, M.G.; Zhou, J.; Malandrino, M.; Sangiorgi, G.; Rizzi, C.; Ferrero, L.; Dommen, J.; Bolzacchini, E. PM chemical composition and oxidative potential of the soluble fraction of particles at two sites in the urban area of Milan, Northern Italy. *Atmos. Environ.* **2016**, *128*, 104–113. [[CrossRef](#)]
45. Tsakiri, M.; Grigoratos, T.; Samara, C. Redox activity of airborne particulate matter in Thessaloniki Greece in relation to chemical aerosol components. In Proceedings of the 16th International MESAEP Symposium, Ioannina, Greece, 24–27 September 2011.
46. Geller, M.D.; Ntziachristos, L.; Mamakos, A.; Samaras, Z.; Schmitz, D.A.; Froines, J.R.; Sioutas, C. Physicochemical and redox characteristics of particulate matter (PM) emitted from gasoline and diesel passenger cars. *Atmos. Environ.* **2006**, *40*, 6988–7004. [[CrossRef](#)]
47. Charrier, J.G.; Richards-Henderson, N.K.; Bein, K.J.; McFall, A.S.; Wexler, A.S.; Anastasio, C. Oxidant production from source-oriented particulate matter-Part 1: Oxidative potential using the dithiothreitol (DTT) assay. *Atmos. Chem. Phys.* **2015**, *15*, 2327–2340. [[CrossRef](#)]
48. Mugica, V.; Ortiz, E.; Molina, L.; De Vizcaya-Ruiz, A.; Nebot, A.; Quintana, R.; Aguilar, J.; Alcantara, E. PM composition and source reconciliation in Mexico City. *Atmos. Environ.* **2009**, *43*, 5068–5074. [[CrossRef](#)]
49. Jeng, H.A. Chemical composition of ambient particulate matter and redox activity. *Environ. Monit. Assess.* **2010**, *169*, 597–606. [[CrossRef](#)] [[PubMed](#)]
50. Hu, S.; Polidori, A.; Arhami, M.; Shafer, M.M.; Schauer, J.J.; Cho, A.; Sioutas, C. Redox activity and chemical speciation of size fractionated PM in the communities of the Los Angeles-Long Beach harbor. *Atmos. Chem. Phys.* **2008**, *8*, 6439–6451. [[CrossRef](#)]
51. Fang, T.; Zeng, L.; Gao, D.; Verma, V.; Stefaniak, A.B.; Weber, R.J. Ambient Size Distributions and Lung Deposition of Aerosol Dithiothreitol-Measured Oxidative Potential: Contrast between Soluble and Insoluble Particles. *Environ. Sci. Technol.* **2017**, *51*, 6802–6811. [[CrossRef](#)] [[PubMed](#)]
52. Biswas, S.; Verma, V.; Schauer, J.J.; Cassee, F.R.; Cho, A.K.; Sioutas, C. Oxidative potential of semi-volatile and non volatile particulate matter (PM) from heavy-duty vehicles retrofitted with emission control technologies. *Environ. Sci. Technol.* **2009**, *43*, 3905–3912. [[CrossRef](#)] [[PubMed](#)]
53. Fang, T.; Verma, V.; Guo, H.; King, L.E.; Edgerton, E.S.; Weber, R.J. A semi-automated system for quantifying the oxidative potential of ambient particles in aqueous extracts using the dithiothreitol (DTT) assay: results from the Southeastern Center for Air Pollution and Epidemiology (SCAPE). *Atmos. Meas. Tech.* **2015**, *8*, 471–482. [[CrossRef](#)]
54. Reid, J.S.; Koppmann, R.; Eck, T.F.; Eleuterio, D.P. A review of biomass burning emissions part II: Intensive physical properties of biomass burning particles. *Atmos. Chem. Phys.* **2005**, *5*, 799–825. [[CrossRef](#)]
55. Saarikoski, S.; Timonen, H.; Saarnio, K.; Aurela, M.; Jarvi, L.; Keronen, P.; Kerminen, V.-M.; Hillamo, R. Sources of organic carbon in fine particulate matter in northern European urban air. *Atmos. Chem. Phys.* **2008**, *8*, 6281–6295. [[CrossRef](#)]
56. Saffari, A.; Daher, N.; Samara, C.; Voutsas, D.; Kouras, A.; Manoli, E.; Karagkiozidou, O.; Vlachokostas, C.; Moussiopoulos, N.; Shafer, M.M.; et al. Increased Biomass Burning Due to the Economic Crisis in Greece and Its Adverse Impact on Wintertime Air Quality in Thessaloniki. *Environ. Sci. Technol.* **2013**, *47*, 13313–13320. [[CrossRef](#)] [[PubMed](#)]
57. Chrysikou, L.P.; Samara, C.A. Seasonal variation of the size distribution of urban particulate matter and associated organic pollutants in the ambient air. *Atmos. Environ.* **2009**, *43*, 4557–4569. [[CrossRef](#)]
58. Zhang, Y.; Yang, B.; Gan, J.; Liu, C.; Shu, X.; Shu, J. Nitration of particle associated PAHs and their derivatives (nitro-, oxy-, and hydroxy-PAHs) with NO<sub>3</sub> radicals. *Atmos. Environ.* **2011**, *45*, 2515–2521. [[CrossRef](#)]
59. Van Drooge, B.L.; Grimalt, J.O. Particle size-resolved source apportionment of primary and secondary organic tracer compounds at urban and rural locations in Spain. *Atmos. Chem. Phys.* **2015**, *15*, 7735–7752. [[CrossRef](#)]

60. Pietrogrande, M.C.; Bacco, D.; Visentin, M.; Ferrari, S.; Poluzzi, V. Polar organic marker compounds in atmospheric aerosol in the Po Valley during the Supersito campaigns-Part 1: Low molecular weight carboxylic acids in cold seasons. *Atmos. Environ.* **2014**, *48*, 164–175. [[CrossRef](#)]
61. Verma, V.; Polidori, A.; Schauer, J.J.; Shafer, M.M.; Cassee, F.R.; Sioutas, C. Physicochemical and toxicological profiles of particulate matter in Los Angeles during the October 2007 Southern California wildfires. *Environ. Sci. Technol.* **2009**, *43*, 954–960. [[CrossRef](#)] [[PubMed](#)]
62. Chung, M.Y.; Lazaro, R.A.; Lim, D.; Jackson, J.; Lyon, J.; Rendulic, D.; Hasson, A.S. Aerosol-borne quinones and reactive oxygen species generation by particulate matter extracts. *Environ. Sci. Technol.* **2006**, *40*, 4880–4886. [[CrossRef](#)] [[PubMed](#)]
63. Cheung, K.L.; Ntziachristos, L.; Tzamkiozis, T.; Schauer, J.J.; Samaras, Z.; Moore, K.F.; Sioutas, C. Emissions of Particulate Trace Elements, Metals and Organic Species from Gasoline, Diesel, and Biodiesel Passenger Vehicles and Their Relation to Oxidative Potential. *Aerosol Sci. Technol.* **2010**, *44*, 500–513. [[CrossRef](#)]



© 2017 by the author. Licensee MDPI, Basel, Switzerland. This article is an open access article distributed under the terms and conditions of the Creative Commons Attribution (CC BY) license (<http://creativecommons.org/licenses/by/4.0/>).